

Coherent exciton states of excitonic nanocrystal-molecules

Suc-Kyoung Hong and Seog Woo Nam

Department of Display and Semiconductor Physics, Korea University, Seochang, Jochiwon, Chungnam 339-700, Korea

Kyu-Hwang Yeon

Department of Physics, College of Natural Science, Chungbuk National University, Cheonju, Chungbuk 361-763, Korea

(Received 19 January 2007; revised manuscript received 12 March 2007; published 24 September 2007)

Coherent exciton states in a nanocrystal-molecule consisting of closely spaced semiconductor nanocrystals have been studied theoretically with a simple resonant dipole-dipole interaction model. In this study, it has been considered that a nanocrystal-molecule is coupled with a photon which is resonant with an exciton in a nanocrystal. The configurations of nanocrystal-molecule considered here are a dimer and a triangular trimer. The eigen-wave-functions and eigenenergies of a nanocrystal dimer molecule and a nanocrystal triangular trimer molecule are obtained. The exciton population dynamics in the dimer and the triangular trimer system is analyzed by obtaining the diagonal elements of the density matrix for several specified initial excitation conditions of nanocrystals as well. In addition, the correlation between nanocrystals in a nanocrystal-molecule is analyzed through obtaining the off-diagonal elements of the density matrix. In the nanocrystal-molecule with the resonant energy transfer model, the energy transfer via dipole-dipole interaction enforces the interference between exciton waves generated in the nanocrystal-molecular systems.

DOI: [10.1103/PhysRevB.76.115330](https://doi.org/10.1103/PhysRevB.76.115330)

PACS number(s): 73.23.-b, 71.35.-y, 78.67.Bf, 42.50.Ct

I. INTRODUCTION

Advances in the fabrication of nanoscale semiconductor structures allow artificial composition of nanocrystal (NC)-molecules, where the optical and electronic properties of the NC-molecules can be controlled by their inter-NC distance, composition, configurational variance, and relative orientation of transition dipole moment. The quantum coherence is one of the important themes in nanoscale systems, since it enables study of fundamental phenomena in nanoscale world and has promising applications for quantum information processing. In order to see the effects of the quantum coherence in a quantum dot array, carrier transport in quantum dot dimer has been studied much both in theoretical and experimental aspects.¹⁻⁷ Rokhinson studied the coherence of charge transfer through a weakly coupled double-dot dimer; one of the dots is strongly coupled to leads.¹ The transport spectra of a quantum dot dimer² and the conductance through two quantum dots connected in a series were examined below the Kondo temperature as a function of the gate voltage³ by Aono *et al.* To show the external field effect on the quantum coherence, Taut *et al.* investigated the time evolution of initially localized states in two-dimensional quantum dot arrays in a magnetic field.⁸ Interference effects in the conductance of multilevel quantum dots were also studied.⁹ Besides, the entanglement of a quantum dot dimer or array through excitation energy transfer via dipole-dipole coupling was considered as well.¹⁰ When the NCs of the molecule are in close proximity but are prevented from direct carrier hopping by surface passivation, they are strongly coupled with each other via dipole-dipole interaction. In such quantum dot or NC aggregates, the exciton hopping is enforced by the energy transfer via resonance dipole-dipole interaction (RDDI).^{11,12} Through the approach of the excitation energy transfer via dipole-dipole coupling, the dynamics of excitonic states in dimer and trimer arrangements of colloidal quantum dots and their extended coherent exciton states in

quantum dot arrays was studied.^{13,14} In the process of the exciton hopping, there has been consideration of the question of the wavelike feature of the exciton motion.^{15,16}

We are interested in coherent exciton states in a nanocrystal-molecule consisting of closely spaced surface passivated semiconductor NCs, where the NCs are assumed to be coupled with each other via strong dipole-dipole interaction without direct carrier hopping between NCs. In this study, it is considered that a nanocrystal-molecule is coupled with a photon which is resonant with an exciton in an NC. The transition frequency of an exciton in an NC of an NC-molecule is also assumed to be one of a cavity (defect) mode inside the photonic band gap (PBG) of the material surrounding the NC-molecule. The configuration of a nanocrystal-molecule considered here is a dimer. The configuration of a triangular trimer is also considered for comparison. The eigen-wave-functions and eigenenergies of a nanocrystal dimer molecule and a nanocrystal triangular trimer molecule are obtained. The exciton population dynamics in the dimer and the triangular trimer system is analyzed by obtaining the diagonal elements of the density matrix for several specified initial excitation conditions of nanocrystals as well. In addition, the correlation between nanocrystals in a nanocrystal-molecule is analyzed through obtaining the off-diagonal elements of the density matrix. In the nanocrystal-molecule in the resonant energy transfer model, the energy transfer via dipole-dipole interaction generates propagating exciton waves which interfere with each other. In this work, we consider the general feature of the coherence properties of exciton dynamics in a dimer NC-molecule and a triangular trimer NC-molecule which are each coupled with a photon. In the calculation of the excitation transport, a simple dipole-dipole coupling model is employed. The next section describes the model and methods. Sections III and IV deal with the eigen-wave-functions, eigenenergies, and coherent exciton dynamics of a dimer NC-molecule and a triangular trimer NC-

molecule, respectively. Summary and discussions are given in Sec. V.

II. MODEL AND METHODS

An excited NC in an NC aggregate interacts with other NCs via both longitudinal and transverse fields. The excitation transport in the surface passivated NC aggregate is different from electronic transport in that there is no net transport of charge which is inhibited due to the passivation of the surface of NCs. When the distance between NCs is much smaller than the electronic-energy-transition wavelength of the excitation, the excitation transport is explained by the instantaneous direct longitudinal Coulomb coupling, i.e., RDDI between the virtual electromagnetic field generated by the transition dipoles of resonant transitions in an excited donor NC and the polarization of a ground-state acceptor NC. The dipole-dipole coupling energy J between the i th and j th NCs with orientational factor κ is $J_{ij} \propto \mu_i \mu_j \kappa_{ij} / \epsilon R_{ij}^3$, where μ is the magnitude of the transition dipole moment of an NC, ϵ is the dielectric constant of the surrounding medium, and R is the inter-NC separation.

In this section, we employ a simple model for a nanocrystal aggregate consisting of two or three NCs which are Coulomb coupled with each other and also coupled to a photon. Meanwhile, it is well known that the Jaynes-Cummings model can be extended to include dipole-dipole interaction between atoms,¹⁷ where Jaynes-Cummings model consists of two-level atoms with a single-mode field in a lossless cavity.¹⁸ The Hamiltonian of the extended Jaynes-Cummings model for the description of the system considered here is given by

$$\hat{H} = \frac{1}{2} \sum_i \omega_i \sigma_i^z + \omega \hat{a}^\dagger \hat{a} + \sum_{i \neq j} (J_{ij} \sigma_i^\dagger \sigma_j + g_{\vec{k}} e^{i\vec{k} \cdot \vec{r}_i} \sigma_i^\dagger a + \text{H.c.}), \quad (1)$$

where $\hbar=1$ for convenience, ω_i and ω are the excitonic energies of the i th NC and the photon, respectively, J_{ij} is the Coulomb coupling described above, $g_{\vec{k}} = \sqrt{2\pi\hbar\omega/V\hat{\epsilon} \cdot \vec{\mu}_i(\vec{r}_i)}$ is the i th NC-radiation coupling constant, V is the volume of the cavity mode, and \vec{r}_i is the position of the i th NC. Here, the set of 2×2 Pauli operators is employed to investigate the quantum dynamics of the two-level NCs, where σ_i^z , σ_i^\dagger , and σ_i describe inversion, excitation, and de-excitation of the i th NC, respectively. \hat{a} and \hat{a}^\dagger are the annihilation and the creation operators, respectively, for photon in the mode \vec{k} , which is the wave vector of the photon. In this study, however, we consider the case with separation between NCs to be much smaller than the wavelength of the excitonic transition energy, where the main channel of the exciton hopping is RDDI and retarded interactions are ignored. Moreover, the transition wavelength of the NCs of an NC-molecule is assumed to be a cavity (defect) mode in photonic band gap material and be in the stop band of the surrounding PBG structure. For simplicity, we consider single excitation in an NC-molecule. For an NC-molecule of N (two or three) nanocrystals coupled with a photon, there are $N+1$ states which span the whole system. The basis state represented by $|j\rangle$ is

defined as only the j th NC is excited, other NCs are unexcited, and no photon exists. $|0\rangle$ is used for the expression of the state that one photon is present and all NCs are unexcited. Then, the total wave function of the Hamiltonian \hat{H} can be written as

$$|\psi(t)\rangle = \sum_{j=0}^N c_j(t) |j\rangle. \quad (2)$$

The eigenstates $|\phi_m\rangle$ of an NC-molecule are obtained simply from the eigenvalue equation $\hat{H}|\phi_m\rangle = \lambda_m |\phi_m\rangle$, with eigenenergies $\lambda = \{\lambda_m\}$ for the Hamiltonian \hat{H} of Eq. (1).

For the analysis of the excitation dynamics of the system, the method of time evolution of density operator is employed. For a given Hamiltonian, the density operator $\hat{\rho}(t)$ in the Heisenberg representation is written as

$$\hat{\rho}(t) = \exp(i\hat{H}t) \hat{\rho}(0) \exp(-i\hat{H}t), \quad (3)$$

where $\hat{\rho}(0)$ is the initial density operator. When \hat{H} can be diagonalized, i.e., if we can find U such that $\hat{H} = UDU^{-1}$, where D is a diagonalized matrix, and if we can define

$$\exp(\hat{H}) \equiv U \exp(D) U^{-1}, \quad (4)$$

with

$$U = (\hat{e}_1, \dots, \hat{e}_N), \quad (5)$$

where \hat{e}_j is j th eigenvector of the Hamiltonian \hat{H} , then the density matrix [Eq. (3)] is expressed as

$$\hat{\rho}(t) = \sum_{\alpha, \gamma} e^{i(\lambda_\alpha - \lambda_\gamma)t} U |\alpha\rangle \langle \alpha | \hat{\rho}_U | \gamma\rangle \langle \gamma | U^{-1}, \quad (6)$$

where λ_j is the eigenvalue of the Hamiltonian \hat{H} for the eigenstate $|j\rangle$, and $\hat{\rho}_U = U^{-1} \hat{\rho}(0) U$. Thus, the matrix elements of the density operator are given by

$$\hat{\rho}_{nm}(t) = \sum_{\alpha, \gamma} e^{i(\lambda_\alpha - \lambda_\gamma)t} U_{n\alpha} (\hat{\rho}_U)_{\alpha\gamma} (U^{-1})_{\gamma m}. \quad (7)$$

The probability of the j th NC being excited is represented as

$$n_j(t) = \rho_{jj}(t), \quad (8)$$

where $j=1, 2, \dots, N$. When $j=0$ in Eq. (8), it is the expected number of photon in the system, i.e., $n_0(t)$ is the average photon number of the NC-molecular system. The correlation between two NCs, or one NC and the photon field, is given by the off-diagonal elements of density operator $\rho_{ij}(t)$.

III. NC-DIMER COUPLED WITH A SINGLE-MODE PHOTON

A dimer NC-molecule ($N=2$) coupled with a photon in a defect of a PBG structure is considered in this section. When NCs are identical, inter-NC distance is much smaller than the transition wavelength, and the photon is resonant with NC; the eigenstates $|\phi_m\rangle$ of the system are given by

$$\begin{aligned}
 |\phi_1\rangle &= \frac{1}{\sqrt{2}} \begin{pmatrix} 0 \\ -1 \\ 1 \end{pmatrix}, & |\phi_2\rangle &= \frac{\sqrt{2}r}{\sqrt{s^2-s}} \begin{pmatrix} \frac{s-1}{2r} \\ 1 \\ 1 \end{pmatrix}, \\
 |\phi_3\rangle &= \frac{\sqrt{2}r}{\sqrt{s^2+s}} \begin{pmatrix} -\frac{s+1}{2r} \\ 1 \\ 1 \end{pmatrix},
 \end{aligned} \quad (9)$$

with energy eigenvalues λ_m ,

$$\lambda = \left\{ \omega - J, \omega + \frac{s+1}{2}J, \omega - \frac{s-1}{2}J \right\}, \quad (10)$$

where $g_{\bar{k}}=g$, $J_{12}=J$, $r=g/J$, and $s=\sqrt{1+8r^2}$. The first element of an eigenvector is for the photon field, and the second and the third elements are for the NCs at sites "1" and "2," respectively. When there is no NC-photon coupling, i.e., $g=0$, the system corresponds to a dipole-dipole coupled dimer. In that case, $|\phi_1\rangle$ and $|\phi_2\rangle$ are the so-called subradiant and superradiant states whose corresponding energy eigenvalues are $\omega-J$ and $\omega+J$, respectively,¹⁹⁻²² and $|\phi_3\rangle$ is a photon state with energy eigenvalue ω , as expected, i.e.,

$$|\phi_1\rangle = \frac{1}{\sqrt{2}} \begin{pmatrix} 0 \\ -1 \\ 1 \end{pmatrix}, \quad |\phi_2\rangle = \frac{1}{\sqrt{2}} \begin{pmatrix} 0 \\ 1 \\ 1 \end{pmatrix}, \quad |\phi_3\rangle = \begin{pmatrix} 1 \\ 0 \\ 0 \end{pmatrix}. \quad (11)$$

When there is no Coulomb coupling between NCs, i.e., $J=0$, the eigenstates are expressed as

$$|\phi_1\rangle = \frac{1}{\sqrt{2}} \begin{pmatrix} 0 \\ -1 \\ 1 \end{pmatrix}, \quad |\phi_2\rangle = \frac{1}{2} \begin{pmatrix} \sqrt{2} \\ 1 \\ 1 \end{pmatrix}, \quad |\phi_3\rangle = \frac{1}{2} \begin{pmatrix} -\sqrt{2} \\ 1 \\ 1 \end{pmatrix}, \quad (12)$$

with energy eigenvalues $\lambda = \{\omega, \omega + \sqrt{2}g, \omega - \sqrt{2}g\}$. These are just for the model of the collective spontaneous emission proposed by Cummings *et al.*¹⁸ Equation (12) indicates that an excitation is shared by two NCs only, or it is shared by a photon field and two NCs either in a symmetric or antisymmetric fashion.

As for the dynamics of coherent exciton and photon number, we obtain the matrix elements of the density operator $\hat{\rho}(t)$ for several specified initial excitation conditions. Under the initial condition $\rho_{lm}(0) = \delta_{l0}\delta_{m0}$, that is, initially when one photon present and no NC is excited, the matrix elements of the density matrix $\hat{\rho}(t)$ is yielded to

$$n_0(t) = 1 - \frac{8r^2}{s^2} \cos^2 \frac{Jst}{2}, \quad (13)$$

$$n_1(t) = \frac{4r^2}{s^2} \sin^2 \frac{Jst}{2}, \quad (14)$$

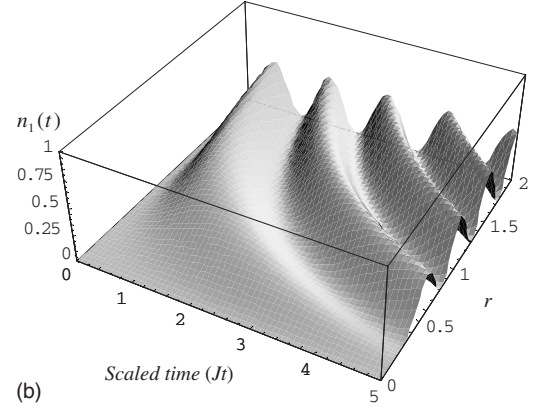
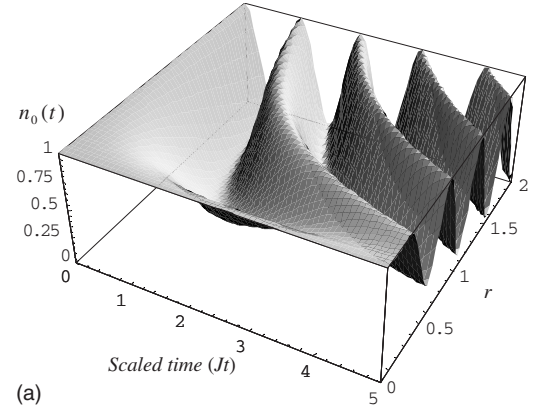


FIG. 1. The expected photon number $n_0(t)$ and exciton population $n_1(t)$ as functions of scaled time Jt and r are plotted in (a) and (b), respectively. The initial condition is $\rho_{kl}(0) = \delta_{kl}\delta_{k0}$.

$$\rho_{01}(t) = -\frac{r}{s^2} (\cos Jst - is \sin Jst), \quad (15)$$

$n_2(t) = n_1(t)$, $\rho_{02}(t) = \rho_{01}(t)$, and $\rho_{12}(t) = n_1(t)$. The diagonal elements of the density matrix $\hat{\rho}(t)$ show the dynamics of the coherent excitonic state, and the off-diagonal matrix elements of $\hat{\rho}(t)$ carry the information of the dynamical correlation of the excitations between two NCs or the photon field and the excitation of an NC. The probabilities of the photon number and the excitation population in NCs are shown in Fig. 1 as functions of Jt and r . For the estimation of the typical time scales of exciton dynamics, the typical values of the couplings for realistic NCs in a nanocavity of a PBG structure, J and g , are required. The typical Coulomb coupling energy between close NCs with inter-NC distance of $R \sim 100 \text{ \AA}$ is $J \sim 0.1 \text{ meV}$ for the transition dipole moment of $\mu \sim 10 \text{ D}$ without considering the orientational factor and the dielectric effect.¹⁶ For the NC-radiation coupling, typically, in a nanocavity of a PBG structure at optical frequency, $g \sim 0.01 \text{ meV}$ for the transition dipole moment of $\mu \sim 10 \text{ D}$ and the mode volume of $V \sim 1 \text{ \mu m}^3$.²³ In practice, the coupling energies J and g could be (partly) controlled by varying the relative orientation of transition dipoles and the polarization of the light. For these typical values, the scaled time $Jt=1$ corresponds to $\sim 5 \text{ ps}$. Figures 1(a) and 1(b) are for the number of photons and the excitation population of an NC,

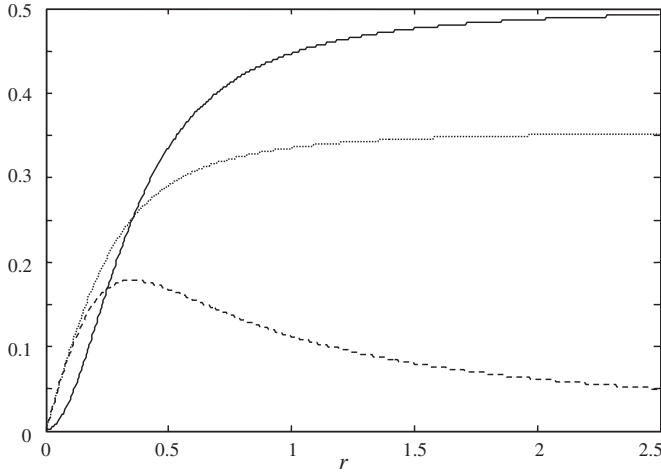


FIG. 2. Dependence of $4r^2/s^2$, r/s^2 , and r/s on r is plotted in solid, dashed, and dotted lines, respectively.

respectively. The initial energy of the photon field is partly transferred to NCs and the transferred energy moves back and forth with angular frequency Js . The frequency is proportional to s and the highest excitation population of NC is given by $4r^2/s^2$, whose asymptotic value is 0.5 in the limit of $r \gg 1$. The prohibition of the complete transfer of the field energy to NC-molecule comes from the Coulomb coupling of two NCs.²² The correlation between the photon field and the excitation of an NC oscillates with maximum amplitude r/s^2 , whereas the correlation between two NCs oscillates with maximum $4r^2/s^2$ both at angular frequency Js . In order to see the dependence of the amplitudes of $n_0(t)$, $n_1(t)$, $\rho_{01}(t)$, and $\rho_{12}(t)$ on the parameter r , $4r^2/s^2$ (solid line) and r/s^2 (dashed line) are plotted as functions of r as shown in Fig. 2. The maximum of the dashed curve occurs at $r=1/2\sqrt{2}$. The dotted curve is for r/s , which shows up in the following equations.

Now, under the initial condition $\rho_{lm}(0)=\delta_{l1}\delta_{m1}$, that is, initially when the first NC is excited, the second NC unexcited, and there is no photon present, the matrix elements of the density matrix $\hat{\rho}(t)$ reduce to

$$n_0(t) = \frac{4r^2}{s^2} \sin^2 \frac{1}{2} Jst, \quad (16)$$

$$n_1(t) = \frac{1}{8s^2} \left[4(-s + 2r^2) \sin \frac{3Jt}{2} \sin \frac{Jst}{2} + 4(s^2 + 2r^2) \cos \frac{3Jt}{2} \cos \frac{Jst}{2} + 1 + 3s^2 \right], \quad (17)$$

$$n_2(t) = \frac{1}{8s^2} \left[4(s + 2r^2) \sin \frac{3Jt}{2} \sin \frac{Jst}{2} + 4(-s^2 + 2r^2) \cos \frac{3Jt}{2} \cos \frac{Jst}{2} + 1 + 3s^2 \right], \quad (18)$$

$$\rho_{01}(t) = \frac{r}{2s^2} (1 - \cos Jst + is \sin Jst) - \frac{r}{s} \left(\sin \frac{3Jt}{2} - i \cos \frac{3Jt}{2} \right) \sin \frac{Jst}{2}, \quad (19)$$

$$\rho_{02}(t) = \frac{r}{2s^2} (1 - \cos Jst + is \sin Jst) + \frac{r}{s} \left(\sin \frac{3Jt}{2} - i \cos \frac{3Jt}{2} \right) \sin \frac{Jst}{2}, \quad (20)$$

$$\rho_{12}(t) = -\frac{1}{2s^2} \left[2r^2(1 - \cos Jst) + is \cos \frac{3Jt}{2} \sin \frac{Jst}{2} + is^2 \sin \frac{3Jt}{2} \cos \frac{Jst}{2} \right]. \quad (21)$$

The probabilities of the photon number and the excitation population in NCs are shown in Fig. 3 as functions of Jt and r . Figures 3(a)–3(c) are for the number of photon and the excitation populations of NCs at sites 1 and 2, respectively. The initially excited NC transfers its energy to both a photon field and other NC. The initial excitation energy of the first NC moves back and forth between two NCs via interactive mediation of the photon field as seen easily from the replotted curves in Fig. 4. In the figure, $n_0(t)$, $n_1(t)$, and $n_2(t)$ as functions of scaled time Jt for $r=0.5$ are plotted in solid, dashed, and dotted lines, respectively. From the figures, we see that when $J > g$, the transfer of the excitation in the first NC to the second NC is faster than that to the photon field, as expected. The behavior of the average photon number $n_0(t)$ is the same as that of the excitation population of NCs for the initial condition $\rho_{lm}(0)=\delta_{l0}\delta_{m0}$ of Eq. (14). As r increases, the maximum of photon number increases, as seen from the solid line in Fig. 2.

For comparison, when there is no coupling between NCs, i.e., $J=0$, which is the case related to the model of the collective spontaneous emission in the study of Cummings and Dorri,¹⁸ the diagonal matrix elements of the density matrix $\hat{\rho}(t)$ for $\rho_{lm}(0)=\delta_{l0}\delta_{m0}$ reduce to $n_0(t)=\cos^2\sqrt{2}gt$, $n_1(t)=\frac{1}{2}\sin^2\sqrt{2}gt$, and $n_2(t)=n_1(t)$, as expected.¹⁸ Since there is no coupling between NCs, the energy from the photon field is transferred to both NCs and their energy moves back to the photon field with angular frequency of $2\sqrt{2}g$. The initial field is totally absorbed by NCs and the absorbed energy is totally re-emitted back to the field, which is the so-called superradiance. For the initial preparation $\rho_{lm}(0)=\delta_{l1}\delta_{m1}$,¹⁸ $n_0(t)=\frac{1}{2}\sin^2\sqrt{2}gt$, $n_1(t)=\frac{1}{4}(1+\cos\sqrt{2}gt)^2$, and $n_2(t)=\frac{1}{4}(1-\cos\sqrt{2}gt)^2$. In this case, while the initially excited energy in an NC is completely transferred to other NC via interactive mediation of the coupling to the photon field, only part of the initially excited energy in an NC is radiated to the field, whereas especially when there is no NC-photon coupling, i.e., $g=0$, we get the result for a dipole-dipole coupled dimer, as expected. Thus, initially, when one NC (the first NC) is excited, $n_1(t)=\cos^2 Jt$, $n_2(t)=1-\cos^2 Jt$, and $\rho_{12}(t)=-i\cos Jt \sin Jt$.

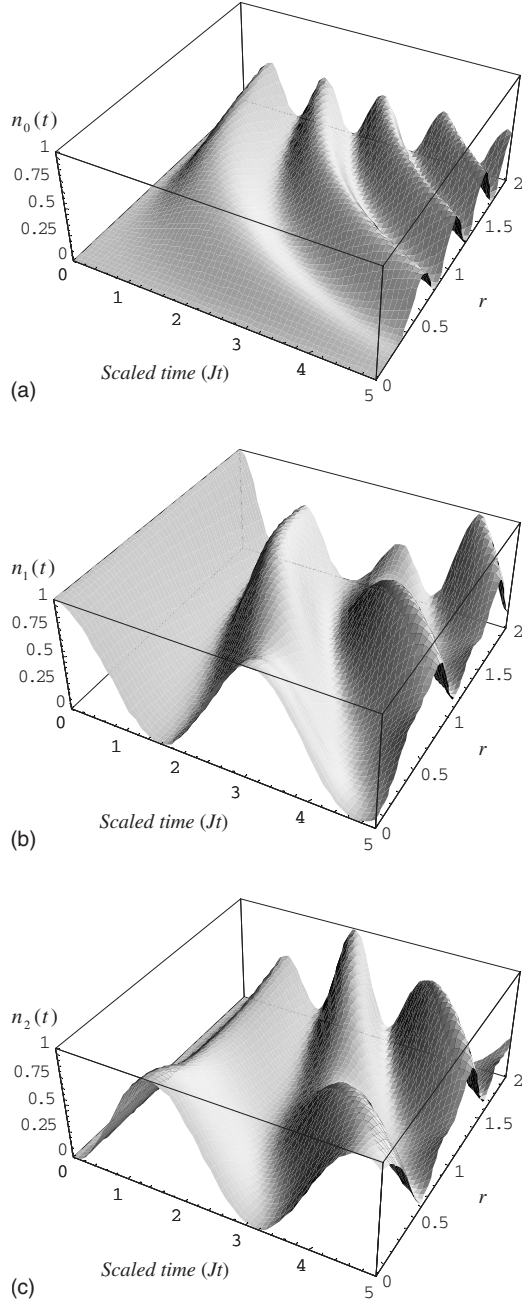


FIG. 3. The expected photon number $n_0(t)$ and exciton populations $n_1(t)$ and $n_2(t)$ as functions of scaled time Jt and r are plotted in (a), (b), and (c), respectively. The initial condition is $\rho_{kl}(0) = \delta_{kl}\delta_{k1}$.

As specified initial preparations, we consider coherently coupled excitations of two NCs. First when two NCs are initially excited in singlet form, i.e., $|\psi(0)\rangle = 1/\sqrt{2}(|1\rangle - |2\rangle)$, the coupled NCs do not emit photon at all, that is, $n_0(t) = 0$ and $n_1(t) = n_2(t) = 1/2$. The off-diagonal elements are $\rho_{12} = -1/2$ and $\rho_{01} = \rho_{02} = -1/2$. The initially prepared state is the so-called subradiant state.^{18,19} Whereas when two NCs are initially in the state of triplet form, i.e., $|\psi(0)\rangle = 1/\sqrt{2}(|1\rangle + |2\rangle)$,

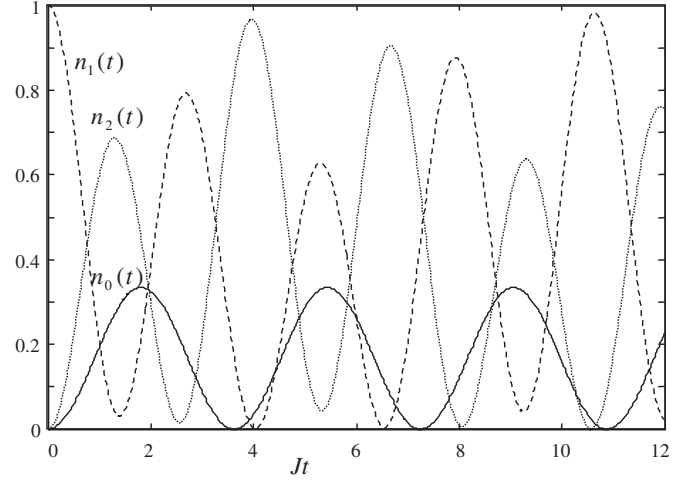


FIG. 4. The photon number $n_0(t)$ and exciton populations $n_1(t)$ and $n_2(t)$ as functions of scaled time Jt for $r=0.5$ are plotted in solid, dashed, and dotted lines, respectively. The initial condition is $\rho_{kl}(0) = \delta_{kl}\delta_{k1}$. The vertical axis is the probability of excitation in NC or photon number.

$$n_0(t) = \frac{8r^2}{s^2} \sin^2 \frac{1}{2} Jst, \quad (22)$$

$$n_1(t) = \frac{1}{2} \left(1 - \frac{8r^2}{s^2} \cos^2 \frac{1}{2} Jst \right), \quad (23)$$

$n_2(t) = n_1(t)$, and $\rho_{12} = n_1(t)$. This result is the reverse of that obtained with the initial condition $\rho_{lm}(0) = \delta_{l0}\delta_{m0}$, i.e., Eqs. (13) and (14). Thus, $n_0(t)$ of Eq. (22) and $n_1(t)$ of Eq. (23) correspond to $2n_1(t)$ of Eq. (14) and $n_0(t)/2$ of Eq. (13), respectively. As $r \gg 1$, $8r^2/s^2$ approaches 1 as seen in Fig. 2, and the excitation energy is totally transferred back and forth. This result comes from the fact that the initially prepared state is the superradiant state.^{18,19}

IV. TRIANGULAR NC-TRIMER COUPLED WITH A SINGLE-MODE PHOTON

In this section, as a specified NC-molecule, a triangular NC ($N=3$) coupled with a photon is considered. When NCs are identical, inter-NC distance is much smaller than the transition wavelength, the photon is resonant with NC, and the Coulomb couplings between NCs are the same; the eigenstates, eigenenergies, and matrix elements of the density operator for the triangular NC-trimer are obtained. From the Hamiltonian of Eq. (1) for the triangular NC-molecule, the eigenstates are simply expressed as

$$|\phi_1\rangle = \frac{1}{\sqrt{2}} \begin{pmatrix} 0 \\ -1 \\ 1 \\ 0 \end{pmatrix}, \quad |\phi_2\rangle = \frac{1}{\sqrt{2}} \begin{pmatrix} 0 \\ -1 \\ 0 \\ 1 \end{pmatrix}, \quad (24)$$

$$|\phi_3\rangle = \frac{r}{\sqrt{2\nu(\nu-1)}} \begin{pmatrix} -\frac{1-\nu}{r} \\ 1 \\ 1 \\ 1 \end{pmatrix},$$

$$|\phi_4\rangle = \frac{r}{\sqrt{2\nu(\nu+1)}} \begin{pmatrix} -\frac{1+\nu}{r} \\ 1 \\ 1 \\ 1 \end{pmatrix}, \quad (25)$$

with the energy eigenvalues λ_m ,

$$\lambda = \{\omega - J, \omega - J, \omega + (1 + \nu)J, \omega + (1 - \nu)J\}, \quad (26)$$

where $g_{\vec{k}} = g$, and $J_{12} = J_{23} = J_{31} = J$, and $\nu = \sqrt{1 + 3r^2}$, with $r = g/J$. The first element of an eigenvector is for the photon field, and the second, the third, and the fourth are for the NCs at sites 1, 2, and 3, respectively. As a reference, when there is no NC-photon coupling, i.e., $g=0$, the system corresponds to a dipole-dipole coupled circular trimer. In that case, the eigenvectors are

$$|\phi_1\rangle = \frac{1}{\sqrt{2}} \begin{pmatrix} 0 \\ -1 \\ 1 \\ 0 \end{pmatrix}, \quad |\phi_2\rangle = \frac{1}{\sqrt{2}} \begin{pmatrix} 0 \\ -1 \\ 0 \\ 1 \end{pmatrix},$$

$$|\phi_3\rangle = \frac{1}{\sqrt{3}} \begin{pmatrix} 0 \\ 1 \\ 1 \\ 1 \end{pmatrix}, \quad |\phi_4\rangle = \begin{pmatrix} 1 \\ 0 \\ 0 \\ 0 \end{pmatrix}, \quad (27)$$

with corresponding energy eigenvalues $\lambda = \{\omega - J, \omega - J, \omega + 2J, \omega\}$, respectively. Here, $|\phi_1\rangle$, $|\phi_2\rangle$, and $|\phi_3\rangle$ are the eigenstates of a circular aggregate of N NCs with only nearest-neighbor interactions, and they are expressed in a simple plane wave form as²⁴

$$|\phi_m\rangle = \frac{1}{\sqrt{N}} \sum_{n=1}^N e^{i2nm\pi/N} |n\rangle, \quad (28)$$

with their corresponding energy eigenvalues λ_m ,

$$\lambda_m = \omega + 2J \cos \frac{2\pi m}{N}, \quad m = 1, 2, \dots, N, \quad (29)$$

and $|\phi_4\rangle$ is a photon state with energy eigenvalue ω , as expected. The degeneracy for a circular aggregate of identical two-level NCs with equidistance is from the rotational symmetry of the excitation in the triangular arrangement of NCs. When there is no Coulomb coupling between NCs, i.e., $J=0$, the eigenstates are expressed as

$$|\phi_1\rangle = \frac{1}{\sqrt{6}} \begin{pmatrix} \sqrt{3} \\ 1 \\ 1 \\ 1 \end{pmatrix}, \quad |\phi_2\rangle = \frac{1}{\sqrt{6}} \begin{pmatrix} -\sqrt{3} \\ 1 \\ 1 \\ 1 \end{pmatrix},$$

$$|\phi_3\rangle = \frac{1}{\sqrt{2}} \begin{pmatrix} 0 \\ -1 \\ 1 \\ 0 \end{pmatrix}, \quad |\phi_4\rangle = \frac{1}{\sqrt{2}} \begin{pmatrix} 0 \\ -1 \\ 0 \\ 1 \end{pmatrix}, \quad (30)$$

with corresponding energy eigenvalues $\lambda = \{\omega + \sqrt{3}g, \omega - \sqrt{3}g, \omega, \omega\}$, respectively.¹⁸ Here, we note that $|\phi_3\rangle$ and $|\phi_4\rangle$ in Eq. (30) differ from $|\phi_1\rangle$ and $|\phi_2\rangle$ in Eq. (27) in that two NCs are not correlated in Eq. (30) whereas two NCs are correlated in Eq. (27); thus, their eigenvalues are different from each other. Equation (30) indicates that an excitation is equally shared by only two NCs among three NCs without photon in antisymmetric fashion, or is shared by a photon field and three NCs either in a symmetric or antisymmetric fashion.

Now, for the analysis of excitation dynamics, the matrix elements of the density operator for several specified initial excitation conditions are evaluated. First, when one photon exists without excitation of any NC, i.e., $\rho_{lm}(0) = \delta_{l0}\delta_{m0}$, the matrix elements of the density operator are expressed as

$$n_0(t) = 1 - \frac{3r^2}{\nu^2} \sin^2 J\nu t, \quad (31)$$

$$n_1(t) = \frac{r^2}{\nu^2} \sin^2 J\nu t, \quad (32)$$

$$\rho_{01}(t) = -\frac{r}{2\nu^2} (1 - \cos 2J\nu t + i\nu \sin 2J\nu t), \quad (33)$$

$n_2(t) = n_3(t) = n_1(t)$, and $\rho_{12}(t) = \rho_{23}(t) = n_1(t)$. The behavior of the probabilities of the photon number and the excitation population in NCs as functions of Jt and r is qualitatively quite similar to that for the dimer NC-molecule shown in Fig. 1. The main difference is the variation time of the dynamics. The characteristic time of the dynamics in trimer NC is shorter than that in dimer NC. The initial energy of the photon field is partly transferred to NCs, and the transferred energy moves back and forth with angular frequency $2J\nu$. The frequency is proportional to ν and the highest excitation population of an NC is given by r^2/ν^2 . In the limit of $r \gg 1$, r^2/ν^2 approaches 0.33 as required.¹⁸ Similar to the case of dimer of Eqs. (13) and (14), the energy initially stored in the photon field does not completely transfer to NCs. The prohibition of the complete transfer of the field energy to NC-molecule comes from the coupling between NCs. The correlation between the photon field and an excitation of an NC oscillates with amplitude proportional to r/ν^2 at angular frequency $2J\nu$, whereas the correlation between two NCs oscillates with maximum amplitude r^2/ν^2 at the same angular frequency $2J\nu$. In order to see the dependence of the amplitudes of $n_0(t)$, $n_1(t)$, $\rho_{01}(t)$, and $\rho_{12}(t)$ on the parameter r , r^2/ν^2 (solid line), r/ν^2 (dashed line), r/ν (dotted line), and

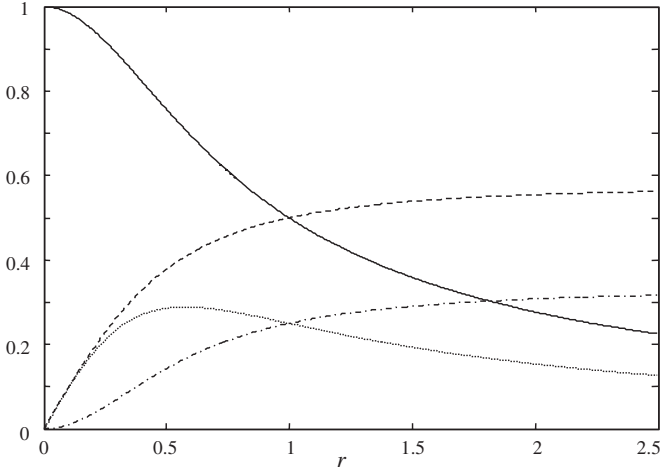


FIG. 5. Dependence of r^2/v^2 , r/v^2 , r/v , and $1/v$ on r is plotted in solid, dashed, dotted, and dashed-dotted lines, respectively.

$1/v$ (dashed-dotted line) are plotted as functions of r , as shown in Fig. 5. The maximum of the dotted curve occurs at $r=1/\sqrt{3}$. In this case, when there is no coupling between NCs, i.e., $J=0$, the matrix elements of the density matrix reduce to $n_0(t)=\cos^2\sqrt{3}gt$, $n_1(t)=\frac{1}{3}\sin^2\sqrt{3}gt$, and $n_2=n_3=n_1(t)$. The initial field energy is completely absorbed by NCs and the absorbed energy is re-emitted back to the field completely as expected in collective absorption of the field in the model of Cummings and Dorri.

For the initial preparation of $\rho_{lm}(0)=\delta_{l1}\delta_{m1}$, the matrix elements of the density matrix are yielded to

$$n_0(t) = \frac{r^2}{v^2} \sin^2 Jvt, \quad (34)$$

$$n_1(t) = \frac{5}{9} - \frac{r^2}{3v^2} \sin^2 Jvt + \frac{4}{9v} (\nu \cos 2Jt \cos Jvt - \sin 2Jt \sin Jvt), \quad (35)$$

$$n_2(t) = \frac{2}{9} - \frac{r^2}{3v^2} \sin^2 Jvt - \frac{2}{9v} (\nu \cos 2Jt \cos Jvt - \sin 2Jt \sin Jvt), \quad (36)$$

$$\rho_{01}(t) = \frac{r}{6v^2} (1 - \cos 2Jvt + i\nu \sin 2Jvt) - \frac{2r}{3v} (\sin 2Jt \sin Jvt - i \cos 2Jt \sin Jvt), \quad (37)$$

$$\rho_{02}(t) = -\frac{r}{6v^2} i \sin Jvt [\nu \cos 2Jt - \nu \cos Jvt + i(\nu \sin 2Jt + \sin Jvt)], \quad (38)$$

$$\rho_{12}(t) = -\frac{1}{9} - \frac{r^2}{3v^2} \sin^2 Jvt - \frac{1}{9v} e^{2iJt} (\nu \cos Jvt + i \sin Jvt) + \frac{2}{9v} e^{-2iJt} (\nu \cos Jvt - i \sin Jvt), \quad (39)$$

$n_3(t)=n_2(t)$, and $\rho_{23}(t)=n_2(t)$. The relation $n_3(t)=n_2(t)$ results from the rotational symmetry. The probabilities of the photon number and the excitation population in NCs are shown in Fig. 6 as functions of Jt and r . Figures 6(a)–6(d) are for the number of photon and the excitation populations of NC at sites 1, 2, and 3, respectively. The behavior of the probabilities of the photon number and the excitation population in NCs as functions of Jt and r is qualitatively not different from that for the dimer shown in Fig. 3. However, there are two main differences; one is the variation time of the dynamics and the other is the degree of transfer of initial energy stored in the first NC for $g=0$, which is described at the end of this section. As for the variation time of the dynamics, it is shorter for the case of trimer than that for the case of dimer. The behavior of the average photon number $n_0(t)$ is the same as that of the excitation population of NCs for the initial condition $\rho_{lm}(0)=\delta_{l0}\delta_{m0}$ of Eq. (32). As r increases, the maximum of photon number increases as seen from the dashed line in Fig. 5. In this case, when $J=0$, the matrix elements of the density matrix are yielded to $n_0(t)=\frac{1}{3}\sin^2\sqrt{3}gt$, $n_1(t)=\frac{1}{9}(2+\cos\sqrt{3}gt)^2$, $n_2(t)=\frac{1}{9}(1-\cos\sqrt{3}gt)^2$, and $n_3=n_2(t)$. The expected photon number and the population probability of the excitation in NCs are replotted in Fig. 7. The photon number $n_0(t)$ and exciton populations in NCs $n_1(t)$, $n_2(t)$, and $n_3(t)$ at sites 1, 2, and 3 as functions of scaled time Jt for $r=0.5$ are plotted in solid, dashed, and dotted lines, respectively. The initially excited energy of the first NC is transferred to other NCs and the photon field but not completely. When there is no NC-photon coupling, i.e., $g=0$, the matrix elements of the density matrix are simply written as $n_1(t)=\frac{1}{9}(5-12\cos Jt+16\cos^3 Jt)$, $n_2(t)=\frac{1}{9}(2+6\cos Jt-8\cos^3 Jt)$, and $n_3=n_2(t)$. From Fig. 6, it is seen that the initial excitation energy of the first NC is only partly transferred to other NCs. The Coulomb coupling interaction between other NCs inhibits complete emission of the initial excitation energy of the first NC.

V. SUMMARY AND DISCUSSIONS

We have studied the dynamics of coherent exciton states in a dimer and a triangular trimer arrangements of colloidal nanocrystals coupled with a single-mode photon field which is resonant with an exciton in a nanocrystal. The separation between NCs was considered to be much smaller than the wavelength of the excitonic transition energy; thus, the main channel of the exciton hopping is RDDI and retarded interactions were ignored. In addition, the transition wavelength of the NCs of an NC-molecule was assumed to be a cavity mode of a nanocavity in a photonic band gap material and therefore be in a stop band of the surrounding PBG structure. On those assumptions, a density matrix approach was employed for the analysis of the dynamics of excitonic states in the NC-molecular systems. The coherent exciton states in an

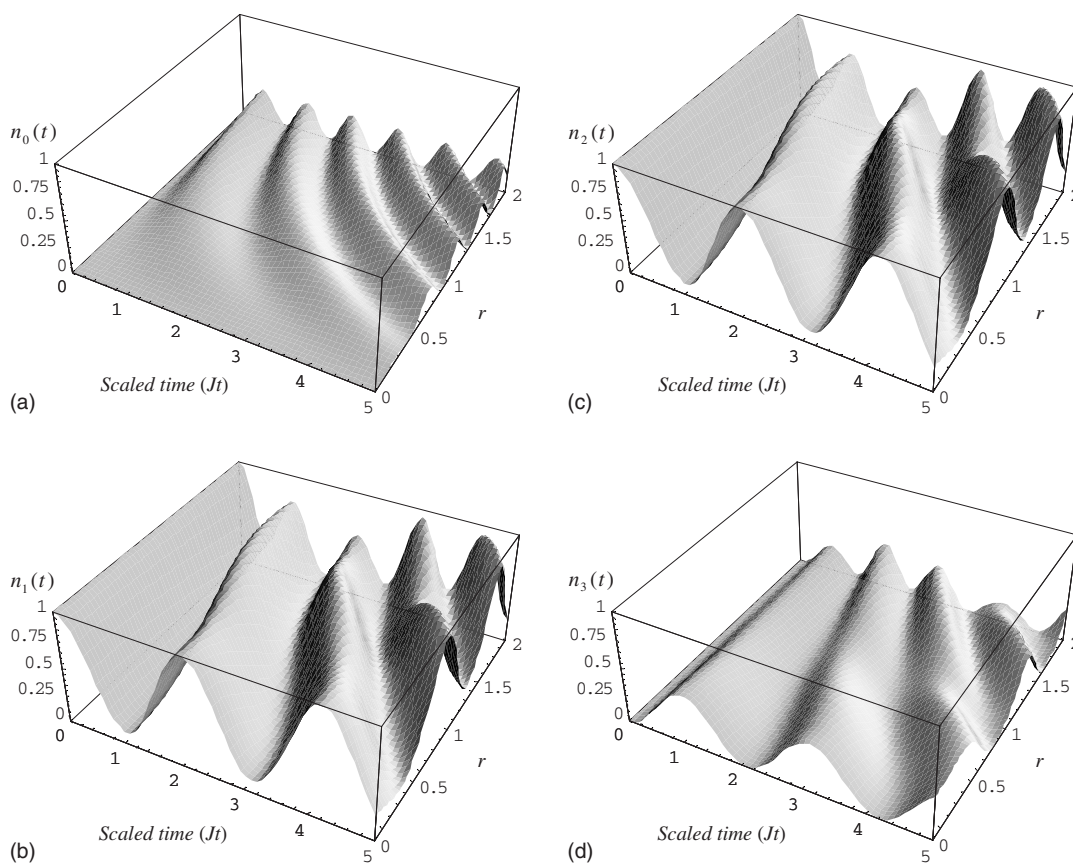


FIG. 6. The expected photon number $n_0(t)$ and exciton populations $n_1(t)$, $n_2(t)$, and $n_3(t)$ as functions of scaled time Jt and r are plotted in (a), (b), (c), and (d), respectively. The initial condition is $\rho_{kl}(0) = \delta_{kl}\delta_{k0}$.

NC-molecule have been studied with a simple resonant dipole-dipole interaction model. The eigen-wave-functions, eigenenergies, and matrix elements of the density operator for several specified initial preparations of the system were obtained for the NC-molecules in order to see the exciton

population dynamics in the dimer and the triangular trimer system.

The experimental realization could be done by implementing a photonic crystal slab nanocavity with a defect whose volume is on the order of $\sim 1 \mu\text{m}^3$.²³ In order to realize a strong coupling between light and NCs in the spacer of photonic crystal nanocavity, a small-volume cavity and atomlike two-level NCs are required. When the defect mode is located in the stop band of the two-dimensional photonic band gap structure, a photon can be trapped in the nanocavity having high Q and small modal volume V . Moreover, NCs have a transition dipole moment much larger than that of an atom, and they could be assembled and fixed in the nanocavity during growth. Optical fiber tips from the vertical side above the photonic crystal could be used for the preparation of the initial excitations. However, one should note that the biexciton effect is not included in our present model. Therefore, a low injection limit is required in the initial excitation. The coherent photon-mediated exciton transfer in the dimer or trimer arrangements of the NCs could also be monitored by other fiber tips from the vertical side below the photonic crystal. Here, the initial excitations and probing of dynamics could be conducted through the irreversible Förster energy transfer. Then, even though the existence of optical fiber tips would affect the coherent oscillations in NC-molecules, it may do so only weakly.

In practice, however, any colloidal quantum dot system in state of the art suffers from strong disorder, which would

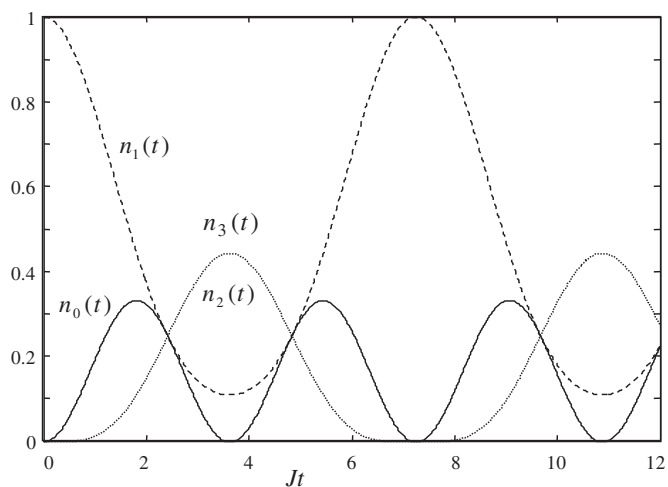


FIG. 7. The photon number $n_0(t)$ and exciton populations $n_1(t)$, $n_2(t)$, and $n_3(t)$ as functions of scaled time Jt for $r=0.5$ are plotted in solid, dashed, and dotted lines, respectively. The initial condition is $\rho_{kl}(0) = \delta_{kl}\delta_{k1}$ and $J=0$. The vertical axis is the probability of excitation in an NC or photon number. Here, $n_3(t) = n_2(t)$.

randomize the couplings, as well as various sources of decoherence that would eventually destroy the coherent oscillations of the density matrix components. There are many sources of disorder and decoherence: the cavity linewidth, the NC exciton linewidth, NC size disparity, the orientational fluctuation of transition dipole moments, the fluctuation in inter-NC distances, and so on. Typically, the intrinsic linewidth of NC exciton is on the order of μeV at low temperature,²⁵ whereas the cavity linewidth is $\sim 100 \mu\text{eV}$. For coherent excitation transfer, smaller inter-NC distance and larger transition dipole moment are desired, since the coupling energy should exceed the decoherence linewidths of both the nanocavity and the NCs. As for the NC size fluctuation which is one of the main source of disorder, the size difference less than that corresponding to the Coulomb coupling energy is required for observing coherent excitation transfer.¹⁶ In NC-trimer case, the fluctuation of the coupling energy due to the randomness of inter-NC distance and relative orientation of transition dipole is also involved into excitation localization. Though the off-diagonal disorder causes relatively weaker localization of exciton than that with the same amount of the diagonal disorder, smaller fluctuation of coupling energy than the average coupling energy is desired as well for observing the coherent feature of the dynamic excitonic states.

In comparison, when NC dimer or trimer is placed on a substrate in free space, which is simpler to implement experimentally, the exciton will interact with a continuum of photon states. Owing to the interaction of NCs with the continuum of photon modes, excited NCs would decay exponentially with oscillation caused by the Coulomb coupling between NCs and the emission of fluorescence photon would be accompanied. In that case, the initially coupled NC exciton state (prepared in the subradiant state) in antisymmetric fashion would be almost nonemissive (in practice, would show slow decay with oscillation).

From the results of the eigen-wave-functions and eigenenergies for a dimer, NC-molecule coupled with a photon in a PBG cavity structure [Eqs. (9) and (10)] can be considered as a three level system for excitonic excitation with constant eigen-wave-functions and eigenenergies for given coupling energies g and J . In practice, however, since the dimer NC-molecule is coupled with a photon, the ac dielectric effect in Coulomb coupling (ϵ in J) varies depending on the presence of the photon field in the system as a function of time $[n_0(t)]$. Then the eigenstates $[|\phi_2\rangle$ and $|\phi_3\rangle$ in Eq. (9)] in which NCs are coupled with a photon would be a function of time. In the absence of interaction between NCs ($J=0$), the model corresponds to that of the collective spontaneous emission proposed by Cummings and Dorri¹⁸ Then, the eigenstates are given such that an excitation is equally shared by two NCs without photon, or the excitation is shared by a photon and two NCs either in symmetric or antisymmetric fashion. Here, the component of the eigenstates for the photon field is \sqrt{N} times bigger than that of the eigenstates for an NC. When we consider the cases without Coulomb coupling and NC-photon coupling separately, it should be noticed that although the shape of the eigenstates in both cases is the same, their corresponding eigenenergies differ from each other, because the NCs in the eigenstates without NC-photon cou-

pling are correlated whereas the NCs in the eigenstates without Coulomb coupling are not correlated. In precise description, $|\phi_1\rangle$ in Eq. (12) differs from $|\phi_1\rangle$ in Eq. (11) in that two NCs are not correlated in Eq. (12) whereas two NCs are correlated in Eq. (11); thus, their eigenvalues are different from each other. The same explanation could be applied to the qualitative description of the eigen-wave-functions and eigenenergies of Eqs. (24), (26), and (30) of the triangular trimer NC-molecule coupled with a photon analyzed in Sec. IV.

In the analysis of the coherent excitation dynamics for a dimer NC-molecule, when one photon initially exists without excitation of any NC, the initial energy which cannot escape the localized area in PBG structure transfers back and forth between a photon field and an NC with angular frequency J_s , but not completely. The prohibition of the complete transfer of the field energy to NCs comes from the coupling of two NCs.²² The degree of the energy transfer increases to its maximum in the limit of $r \gg 1$, as expected. As seen from the dashed curve in Fig. 2, the correlation between the photon field and an NC is maximized when $r = 1/2\sqrt{2} \approx 0.35$.

When the first NC initially is excited, the second NC unexcited, and there is no photon present, the initially excited NC transfers its energy not only to a photon field but also to other NC. The initial excitation energy of the first NC moves back and forth between two NCs via interactive mediation of the photon field as seen from Fig. 3. In this case, it is interesting that the behavior of the average photon number $[n_0(t)]$ is the same as that of NCs' excitation population $[n_1(t)]$ in Eq. (14) obtained with initial condition $|\psi(0)\rangle = |0\rangle$. Especially when $r = g/J = 1$, since the NC-field coupling and the Coulomb coupling are not distinguished in the model Hamiltonian of Eq. (1), the matrix elements of the density operator are the same as those with initial condition $|\psi(0)\rangle = |1\rangle$, except the fact that the role of the photon field in case of $|\psi(0)\rangle = |0\rangle$ is now exchanged with that of the first NC. As r increases, the maximum of photon number increases as seen from the solid line in Fig. 2, as required. When there is no Coulomb coupling ($J=0$), we get the same results as those derived from the model of the collective spontaneous emission in the study of Cummings and Dorri.¹⁸ On the other hand, when there is no NC-photon coupling ($g=0$), we get the result for a dipole-dipole coupled dimer, as expected. As specified initial preparations, coherently coupled initial excitations of two NCs were considered. Then, when two NCs are initially excited in singlet form, the coupled NCs do not emit photon at all, where the initially prepared state is just a subradiant state.¹⁸ When two NCs are initially in the state of triplet form, the initial excitation energy in two NCs is transferred back and forth between a photon field and two NCs, but not completely. The degree of the energy transfer increases to its maximum in the limit of $r \gg 1$, as expected.

The general feature of the results for the triangular trimer NC-molecule coupled with a photon analyzed in Sec. IV is quite similar to that for the dimer NC-molecule coupled with a photon analyzed in Sec. III. Thus, when one photon exists without excitation of NCs, the behavior of exciton population and average photon number $[n_i(t)]$ as functions of Jt and r is qualitatively not different from that for NC-dimer shown

in Fig. 1. The main difference is the variation time of the dynamics. The increased number of couplings between NCs reduces the speed of the variation in the excitation dynamics in trimer compare to that in dimer.¹⁸ Similar to the case of dimer, the energy initially stored in the photon field does not completely transferred to NCs. The prohibition of the complete transfer of the field energy to NC-molecule comes from the coupling between NCs. The correlation between the photon field and an NC oscillates and reaches its maximum at $r=1/\sqrt{3}$. When there is no RDDI coupling ($J=0$), the initial field energy is absorbed completely by NCs and the energy is re-emitted back to the field completely as discussed in the collective absorption of the field in the model of Cummings and Dorri.

Similar to the previous initial preparation, for the initial preparation of $|\psi(0)\rangle=|1\rangle$, the behavior of exciton population and average photon number $[n_j(t)]$ as functions of Jt and r is qualitatively not different from that for NC-dimer shown in Fig. 3. However, there are two peculiar differences: one is the variation time of the dynamics and the other is the degree of energy transfer for no NC-photon coupling ($g=0$). The initially excited energy of the first NC is transferred to other NCs and to the photon field but not completely. Thus, when there is no NC-photon coupling, the initial excitation energy of the first NC is only partly transferred to other NCs as seen

from Fig. 6. The Coulomb coupling interaction between other NCs inhibits complete emission of the initial excitation energy of the first NC.

In summary, we considered coherent exciton states in nanocrystal-molecules consisting of closely spaced semiconductor nanocrystals with a simple resonant dipole-dipole interaction model. In this study, it has been assumed that a nanocrystal-molecule is coupled with a photon which is resonant with an exciton in a nanocrystal. The configurations of nanocrystal-molecule considered here are a dimer and a triangular trimer. The eigen-wave-functions and eigenenergies of a nanocrystal dimer molecule and a nanocrystal triangular trimer molecule were obtained. The exciton population dynamics in the dimer and the triangular trimer system was analyzed by obtaining the diagonal elements of the density matrix for several specified initial excitation conditions of nanocrystals as well. In addition, the correlation between nanocrystals in a nanocrystal-molecule was examined through obtaining the off-diagonal elements of the density matrix. In the nanocrystal-molecules with the resonant energy transfer model, the energy transfer via dipole-dipole interaction enforces interference between exciton waves and generates coherent excitonic states in the nanocrystal-molecular system.

-
- ¹L. P. Rokhinson, L. J. Guo, S. Y. Chou, D. C. Tsui, E. Eisenberg, R. Berkovits, and B. L. Altshuler, *Phys. Rev. Lett.* **88**, 186801 (2002).
- ²K. Kawamura and T. Aono, *Jpn. J. Appl. Phys., Part 1* **36**, 3789 (1997).
- ³T. Aono, M. Eto, and K. Kawamura, *Jpn. J. Appl. Phys., Part 1* **38**, 315 (1999).
- ⁴A. Javier, C. S. Yun, and G. F. Strouse, in *Unconventional Approaches to Nanostructures with Applications in Electronics, Photonics, Information Storage and Sensing*, edited by O. D. Velev, T. J. Bunning, Y. Xia, and P. Yang, MRS Symposia Proceedings No. 776 (Materials Research Society, Pittsburgh, 1999), p. Q.2.1.
- ⁵W. Z. Shangguan, T. C. Au Yeung, Y. B. Yu, and C. H. Kam, *Phys. Rev. B* **63**, 235323 (2001).
- ⁶J. X. Wang, S. Kais, F. Remacle, and R. D. Levine, *J. Phys. Chem. B* **106**, 12847 (2002).
- ⁷Y. Luo, S.-Q. Duan, W.-B. Fan, X.-G. Zao, L.-M. Wang, and B.-K. Ma, *Chin. Phys. Lett.* **19**, 981 (2002).
- ⁸M. Taut, U. Landman, and C. Yannouleas, *Physica E (Amsterdam)* **24**, 308 (2004).
- ⁹C. A. Büsser, G. B. Martins, K. A. Al-Hassanieh, A. Moreo, and E. Dagotto, *Phys. Rev. B* **70**, 245303 (2004).
- ¹⁰Y. N. Chen, D. S. Chuu, and T. Brandes, *Phys. Rev. Lett.* **90**, 166802 (2003).
- ¹¹D. S. Novikov, M. Drndic, L. S. Levitov, M. A. Kastner, M. V. Jarosz, and M. G. Bawendi, *Phys. Rev. B* **72**, 075309 (2005).
- ¹²S. A. Crooker, J. A. Hollingsworth, S. Tretiak, and V. I. Klimov, *Phys. Rev. Lett.* **89**, 186802 (2002).
- ¹³A. N. Al-Ahmadi and S. E. Ulloa, *Phys. Rev. B* **70**, 201302(R) (2004).
- ¹⁴A. N. Al-Ahmadi and S. E. Ulloa, *Appl. Phys. Lett.* **88**, 043110 (2006).
- ¹⁵M. Chachisvilis, O. Kuhn, T. Pullerits, and V. Sundstrom, *J. Phys. Chem. B* **101**, 7275 (1997).
- ¹⁶S.-K. Hong, K. H. Yeon, S. W. Nam, and S. Zhang, *Phys. Lett. A* **360**, 1 (2006).
- ¹⁷S. John and T. Quang, *Phys. Rev. A* **52**, 4083 (1995).
- ¹⁸F. W. Cummings and A. Dorri, *Phys. Rev. A* **28**, 2282 (1983); F. W. Cummings, *ibid.* **33**, 1683 (1986).
- ¹⁹R. H. Dicke, *Phys. Rev.* **93**, 99 (1954).
- ²⁰R. H. Lehberg, *Phys. Rev. A* **2**, 889 (1970).
- ²¹P. S. Lee, Y. C. Lee, and C. T. Chang, *Phys. Rev. A* **8**, 1722 (1973); P. S. Lee and Y. C. Lee, *ibid.* **8**, 1727 (1973).
- ²²K.-C. Liu, *Chin. J. Phys. (Taipei)* **13**, 161 (1975).
- ²³T. Yoshie, A. Scherer, J. Hendrickson, G. Khitrova, H. M. Gibbs, G. Rupper, C. Ell, O. B. Shchekin, and D. G. Deppe, *Nature (London)* **432**, 200 (2004).
- ²⁴A. S. Davydov, *Theory of Molecular Excitons* (Plenum, New York, 1971).
- ²⁵J. P. Reithmaier, G. Sek, A. Löffler, C. Hofmann, S. Kuhn, S. Reitzenstein, L. V. Keldysh, V. D. Kulakovskii, T. L. Reinecke, and A. Forchel, *Nature (London)* **432**, 197 (2004).